

Ultrasonic Attenuation in Antimony. I. Geometric Resonance*†

Y. ECKSTEIN‡§

Department of Physics and Institute for the Study of Metals, University of Chicago, Chicago, Illinois

(Received 11 July 1962)

Geometric resonances in ultrasonic attenuation were observed in antimony. The experimental method used was the continuous method. The sound frequency used was primarily 60 Mc/sec, with some observations at 132 and 252 Mc/sec and magnetic fields 4–200 G. For $q\parallel z$, Shoenberg's carriers were observed and α_{11} determined. For $q\parallel x$ and $q\parallel y$ other highly anisotropic carriers were observed.

INTRODUCTION

WITHIN recent years the investigation of the band structure of metals has been facilitated by the use of magnetoacoustic phenomena as an experimental tool. In this type of experiment, a sound wave of ultrasonic frequencies (12–300 Mc/sec) is sent through a metal and the attenuation of the sound is observed as a function of magnetic field applied perpendicular to the wave vector of the sound. Depending on the magnitude of the field, different effects are observed. At low fields, one expects to find a large increase in attenuation when the sound frequency is an integral multiple of the cyclotron frequency. This effect, which is known as cyclotron resonance, was predicted theoretically,^{1,2} and was found experimentally in gallium.³ Since the magnetic field is low at the frequencies for which techniques are presently available (e.g., 35 G for gallium), the requirement $\omega_c\tau > 1$ is difficult to achieve, and, in fact, cyclotron resonance has been observed only in gallium.

At higher fields, of the order of a few hundred gauss for metals, the attenuation is oscillatory. These oscillations are due to the matching of the diameter of the orbit of the carrier with an integral or half-integral multiple of the wavelength of the sound, and are, therefore, known as geometric resonance. There is, of course, a maximum field above which such behavior cannot occur—when the diameter of the orbit is less than the wavelength of the sound. When these oscillations were first observed,^{4,5} it was immediately realized^{5,6} that the period of the oscillation gives a measure of the extremum momentum of the Fermi surface perpendicular to the sound wave and the magnetic field. This was proved

theoretically,^{2,7–10} and it was shown that the period of oscillation is $\Delta(1/H) = e\lambda/2pc$, where λ is the wavelength of the sound and p is the extremum momentum. This method of investigation of the band structure has already been used for some metals, such as the noble metals^{11,12} and aluminum¹³; and for the semimetal bismuth.¹⁴

The third magnetoacoustic effect which occurs at still higher fields is the de Haas–van Alphen type oscillations,^{14–16} which are found experimentally to be periodic in $1/H$. Reneker¹⁴ observed these oscillations in bismuth and identified them as the type of oscillation found in the diamagnetic susceptibility of conduction electrons (de Haas–van Alphen effect) and in magnetoresistance (de Haas–Shubnikov effect).

In antimony the geometric resonance and de Haas–van Alphen oscillations occur at moderate fields. For 60-Mc/sec sound, geometric resonances were observed at fields up to 100 G; and the de Haas–van Alphen oscillations start at 4000 G.¹⁵ In this paper an experimental investigation of the geometric resonances in antimony will be described.

EXPERIMENTAL METHOD

A single crystal of antimony grown by the Czochralski method was obtained from the Ohio Semiconductor Company. The purity quoted was: impurity content less than 1 ppm. The crystal was oriented by the Laue x-ray method. Since antimony is very brittle, special care must be taken in the preparation of samples in order to avoid straining them. The first sample was cut with an acid string saw, where a mixture of hydrofluoric and nitric acids was used, and the surfaces were made parallel by grinding with a fine powder of carborundum. This method of handling proved to be unsatisfactory, and the remainder of the crystals were cut with a spark cutter and made parallel with a spark planer. The relaxation time of the free carriers, which is a criterion of

* Submitted as a thesis in partial fulfillment of the requirement for the degree of Doctor of Philosophy at the University of Chicago.

† The work was supported in part by a grant from the National Science Foundation to the University of Chicago for research in solid-state properties of bismuth, antimony, and arsenic.

‡ Bell Telephone Predoctoral Fellow and Gulf Oil Predoctoral Fellow.

§ Present address: Argonne National Laboratory, Argonne, Illinois.

¹ N. Mikoshiba, *J. Phys. Soc. Japan* **13**, 759 (1958).

² Morrel H. Cohen, M. J. Harrison, and W. A. Harrison, *Phys. Rev.* **117**, 937 (1960).

³ B. W. Roberts, *Phys. Rev. Letters* **6**, 453 (1961).

⁴ H. E. Bömmel, *Phys. Rev.* **100**, 758 (1955).

⁵ A. B. Pippard, *Phil. Mag.* **2**, 1147 (1957).

⁶ R. W. Morse, H. V. Bohm, and J. D. Gavenda, *Phys. Rev.* **109**, 1394 (1958).

⁷ T. Kjeldaaas and T. Holstein, *Phys. Rev. Letters* **2**, 340 (1959).

⁸ M. Harrison, *Phys. Rev.* **119**, 126 (1960).

⁹ V. L. Gurevich, *Zh. Eksperim. i Teor. Fiz.* **37**, 71 (1959).

¹⁰ A. B. Pippard, *Proc. Roy. Soc. (London)* **A257**, 165 (1960).

¹¹ R. W. Morse, A. Myers, and C. T. Walker, *Phys. Rev. Letters* **4**, 605 (1960).

¹² R. W. Morse and J. D. Gavenda, *Phys. Rev. Letters* **2**, 250 (1959).

¹³ B. W. Roberts, *Phys. Rev.* **119**, 1889 (1960).

¹⁴ D. Reneker, *Phys. Rev.* **115**, 303 (1959).

¹⁵ J. Ketterson, following paper [*Phys. Rev.* **129**, 18 (1963)].

¹⁶ D. Gibbons, *Phil. Mag.* **6**, 445 (1961).

the purity and absence of strain of the crystal, was found to be 10 times larger for these samples than for the mechanically ground crystal. Since all the samples were cut from one large crystal, the purity was the same for all, and any difference in the relaxation time must be attributed to the difference in handling. The relative relaxation times were estimated by the following argument: The lowest magnetic field at which oscillations can be observed is given by $\omega_c\tau > 1$, where ω is the cyclotron frequency ($=eH/m^*c$) and τ is the relaxation time. In the case of the mechanically ground crystal, the oscillations began at a field 10 times greater than for the spark cut crystals, so that the relaxation time was larger by a factor of 10 for these crystals. The mean free path l of the spark cut crystals was estimated to be 1 mm. This estimate was arrived at by using the relation $l = n\lambda$, where λ is the sound wavelength and n is the number of oscillations observed.

In all, four samples were prepared: two with planes perpendicular to the binary axis, one with planes perpendicular to the trigonal axis, and one with planes perpendicular to the bisectrix axis. The planes of the mechanically ground crystal were perpendicular to the binary axis.

Two quartz transducers of 12-Mc/sec stress wave fundamental frequency were attached to the surfaces of the crystal. The bond found to work satisfactorily was Dow Corning 200; and it was found that better results were achieved when the transducer was pressed to the sample by a small weight, in order to make the layer of bond thin and uniform. The sample was suspended directly in liquid helium at the end of two coaxial lines in a standard cryogenic arrangement. At first, Monel tubing was used for the coaxial lines, but it was found that since Monel is slightly ferromagnetic, the magnetic field at the sample was distorted. Therefore, the remainder of the experiments (on the spark-cut crystals) were carried out using stainless steel tubing.

All measurements were taken at 1.2°K. The difference in the amplitude of the oscillations at 1.2 and 4.2°K was large, indicating high purity of the crystal.

For the geometric resonance, the magnetic field, generated by a Helmholtz coil, was low: between 0–23 G. A longitudinal coil and another Helmholtz coil were used in order to cancel the earth's magnetic field. This was done with the help of a Hall probe.

The oscillatory effect itself is small, because of the small number of carriers ($\sim 10^{-3}$ per atom). Therefore, it was almost unobservable by the usual pulse technique, except for a few orientations, in which the last two oscillations before saturation were observed. For this reason, we used the continuous technique^{14,15} in which the derivative of the attenuation is observed. In this method a continuous sound wave is sent through the sample, and a small modulating magnetic field of sinusoidal time dependence is applied in addition to the constant magnetic field. The modulation frequency was 40 cps.

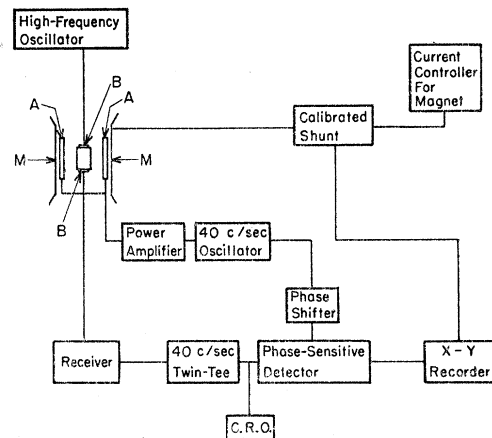


FIG. 1. Block diagram of experiment: A, modulation coils; B, transducer; M, magnet.

The experimental setup was as shown in the block diagram (Fig. 1). The oscillator is a Hewlett-Packard oscillator. The receiver is an A.I.L. 60-Mc/sec i.f. receiver, whose noise figure is 2.3 dB, and which has a 4-Mc/sec bandwidth and fast recovery time. For higher frequency Sage crystal mixes were used. It can also be used for the pulse method, and, indeed, before taking measurements, we used the pulse method to ascertain that the transducer to sample seal did not break while cooling. The x - y recorder used was a Brown x - y recorder.

TABLE I. Velocity of sound at liquid nitrogen temperature.

Longitudinal	$v_x = 3.85 \times 10^5$ cm/sec
Longitudinal	$v_y = 4.08 \times 10^5$ cm/sec
Longitudinal	$v_z = 2.58 \times 10^5$ cm/sec

The velocity of sound (see Table I) was measured by the usual echo technique. The time between echoes was measured by a calibrated delay line. The velocity of sound is given by twice the thickness of the crystal divided by the time between successive echoes. At liquid He temperature the attenuation is very high, and only one echo was observed, the velocity of sound could not be measured at this temperature, and, consequently, it was measured at liquid nitrogen temperature. However, even at this higher temperature, there were only two or three echoes, so that the accuracy is quite low, and is estimated to be about 4%.

THEORY AND RESULTS

For a given sample there exists a minimum sound frequency for which geometric resonances may be observed, because the wavelength cannot be larger than the mean free path, that is, $ql > 1$, for oscillations to occur. It is advantageous to work at higher frequencies, because the period $\Delta(1/H)$ is inversely proportional to frequency, while the maximum field for which oscillations can occur is directly proportional to the frequency;

furthermore, the minimum field for which oscillations can occur is independent of frequency, as will be shown below. Therefore, the number of oscillations which are observed increases with increasing frequency, so that the determination of the period of oscillation becomes more accurate. One can see that the minimum field for which geometric resonances can occur is independent of the frequency (once the condition $ql > 1$ is satisfied), because the carrier must be able to complete an orbit within its mean free path: Therefore, $l \gtrsim r = v_F / \omega_c$, which is equivalent to $\omega_c \tau > 1$. Counteracting the advantages of working at high frequencies is the fact that the attenuation is proportional to the frequency, so that work at high frequencies becomes increasingly difficult. The attenuation also increases strongly as the mean free path increases.

The sample was rotated around the wave vector \mathbf{q} , and measurements were taken at intervals of 10° , starting with one major crystal axis in the direction of the field. The orbit of the carrier does not change when the direction of the magnetic field is reversed. Therefore, an angle of $\theta + 180^\circ$ is equivalent to θ , where θ is the angle between the magnetic field and an arbitrary axis. Therefore, the crystal was rotated only up to 180° with respect to its initial orientation. Two measurements were taken beyond 180° , as a check of the reproducibility of results, and also as a check of the perpendicularity of the wave vector on the magnetic field. The results were reproducible within 1–2%, which is within the experimental error of the determination of the period from the data.

Measurements were made on four samples. For the sample that was cut with an acid string saw and mechanically ground, the background attenuation was not high, and data were taken at 252 Mc/sec, with the sound wave parallel to the binary axis. The mean free path of the remainder of the samples was so long that the attenuation was too high at 250 Mc/sec to detect a signal. It was possible to work up to 132 Mc/sec, but receiver noise was much lower at 60 Mc/sec, so that most of the work on these three samples was done at 60 Mc/sec. These three samples were oriented so that the

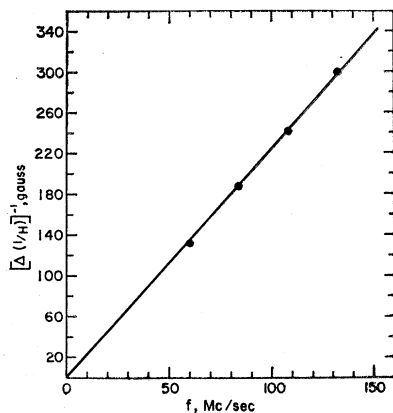


FIG. 2. Period or function of frequency $q \parallel z, H \parallel y$.

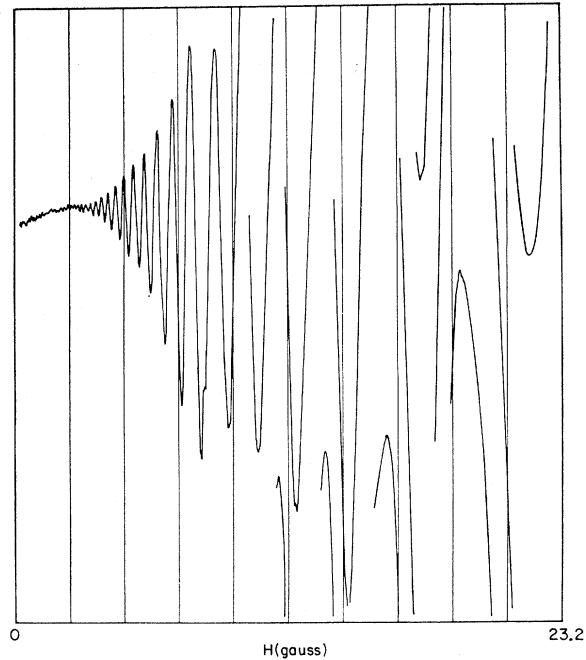


FIG. 3. Experimental curve $q \parallel x$, 60 Mc/sec; H is 66° from y direction.

wave vector was parallel to the binary, trigonal, and bisectrix axes. In the case in which the wave vector was parallel to the trigonal axis, some measurements were made at 132 Mc/sec, and the results were in agreement with the work at 60 Mc/sec. A comparison of the results on the measurements done with the wave vector parallel to the binary axis at 252 and 60 Mc/sec showed that the momentum as a function of angle had the same behavior in both cases, but the momentum measured at 252 Mc/sec was consistently higher by 10%. This is attributed to the distortion of the magnetic field at the sample, due to the Monel tubing, which was replaced by stainless steel tubing for the other samples.

The oscillations were identified as geometric resonances as distinguished from cyclotron resonances and de Haas–van Alphen type oscillations by two criteria: (1) Cyclotron resonance is not an oscillatory phenomenon, but rather a true resonance absorption, which has a different line shape¹⁷; and (2) the period of the de Haas–van Alphen type oscillations is independent of the applied frequency, whereas, in the case of geometric resonance the period $\Delta(1/H)$ is proportional to the wavelength. Figure 2 shows the period $\Delta(1/H)^{-1}$, for one orientation, as a function of the frequency, and, as expected, it is a straight line passing through the origin.

Some examples of the data taken from the x - y recorder are shown in Figs. 3–5. In most orientations, a signal can be detected starting at 4 G (cyclotron reso-

¹⁷ The period of cyclotron resonance scales with reciprocal frequency (instead of wavelength) so use of shear waves in addition to longitudinal waves will distinguish between this phenomenon and geometric resonance in ambiguous cases (reference 3).

nance should occur at about 1 G). Measurements were taken up to 23 G. In this range there were 5–15 oscillations. We did not go to higher fields, although two more oscillations could be recorded before oscillations cease, because these should not be taken into account. The reason is that the oscillatory part of the attenuation behaves roughly as $J(1/H)$, and the Bessel function is periodic only for large arguments; experimentally it was found that the last two oscillations did not follow the periodicity of the other oscillations.

The maxima and minima of the oscillations were plotted as functions of integers and half-integers, respectively, and the slope of the straight line was calculated, giving $\Delta(1/H)$ (see Fig. 6). The extremal momentum p can be calculated from the relation $\Delta(1/H) = e\lambda/2pc$, where the wavelength λ is found by measuring the velocity of sound. The experimental error in the evaluation of $\Delta(1/H)$ from the straight line is 1–5%. This error is due to the uncertainties in reading the

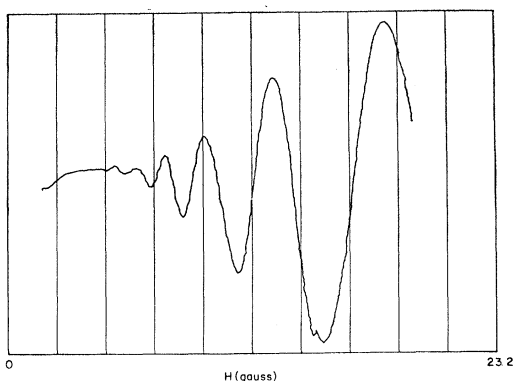


FIG. 4. Experimental curve $q_{\parallel x}$, 252 Mc/sec; H is 37° from z direction.

maxima and minima from the graph; and, more important, because of shifts in the location of the maxima and minima due to interference with other long periods of low amplitude. The probable error in p is thus 7%, because of the added error in λ . The period $\Delta(1/H)$ as a function of angle of the magnetic field in the principal planes is shown in Figs. 7–9. The points are experimental results, and the curve is a fit of the points to an ellipsoidal model discussed later.

Antimony is a semimetal. It is believed that the first five Brillouin zones are filled, and the fifth zone overlaps with the sixth. Thus, a few electrons spill over into the sixth band—the conduction band—and an equal number of holes are created in the fifth band—the valence band. There is experimental evidence^{18,19} that the number of carriers is of the order 10^{-3} electron per atom. For such low carrier density an ellipsoidal Fermi surface may be anticipated. Theoretical work on the band

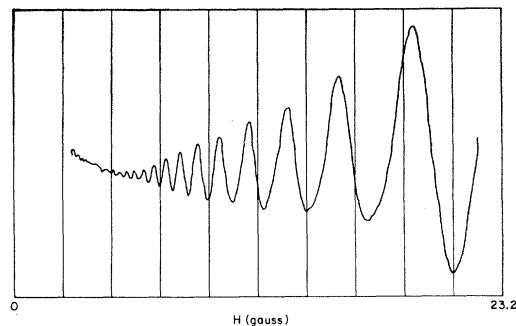


FIG. 5. Experimental curve $q_{\parallel y}$, 60 Mc/sec; H is 16° from x direction.

structure of semimetals²⁰ shows that the Fermi surface should be nearly ellipsoidal. For example, in the case of bismuth (which has only 10^{-5} carrier per atom) the theoretical de Haas–van Alphen period is almost the same as for an ellipsoidal surface in most orientations.²¹

There have only been a few experimental studies made on the band structure of antimony. Shoenberg¹⁷ investigated the de Haas–van Alphen (dHvA) effect in antimony at low temperatures, and interpreted his experimental results by using a model of the Fermi surface consisting of three ellipsoids, whose centers are on the binary axes and which are tilted from the trigonal plane by an angle of 35° . The equation of one ellipsoid is

$$2m_0E = \alpha_{11}p_x^2 + \alpha_{22}p_y^2 + \alpha_{33}p_z^2 + 2\alpha_{23}p_y p_z,$$

and the other two ellipsoids are found by rotating this one by $\pm 120^\circ$ around the z axis; thus the trigonal symmetry of the crystal structure is preserved.

For this band structure the period of oscillation as a function of angle is given by the following formulas:

For $q_{\parallel x}$, $\theta = 0$ is $H_{\parallel z}$ (trigonal axis),

$$\Delta\left(\frac{1}{H}\right)_1 = \frac{e\lambda}{2c(4m_0E)^{1/2}} [(\alpha_{22} + \alpha_{33}) + (\alpha_{22} - \alpha_{33}) \cos 2\theta + 2\alpha_{23} \sin 2\theta]^{1/2}, \quad (1a)$$

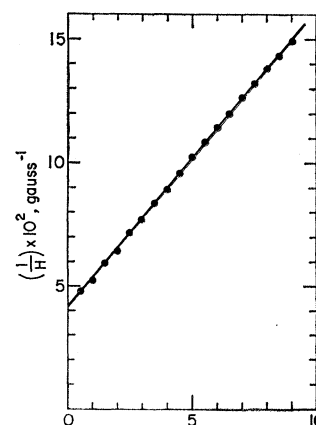


FIG. 6. $\Delta(1/H)$ as function of integer $q_{\parallel y}$, 60 Mc/sec; H is 16° from x direction.

¹⁸ D. Shoenberg, Proc. Roy. Soc. (London) **245**, 1 (1952).

¹⁹ S. J. Freedman and H. J. Juretschke, Phys. Rev. **124**, 1379 (1961).

²⁰ M. H. Cohen, Phys. Rev. **121**, 387 (1961).

²¹ D. Weiner, Phys. Rev. **125**, 1226 (1962).

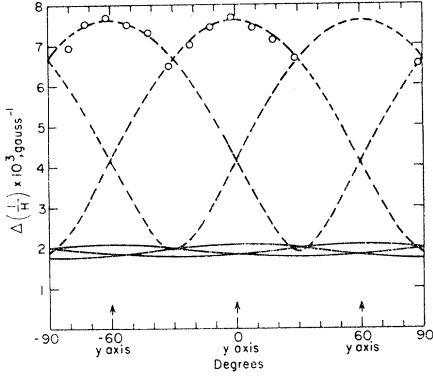


Fig. 7. $\Delta(1/H)$ as function of angle $q||z$; H in xy plane.

$$\Delta\left(\frac{1}{H}\right)_2 = \frac{e\lambda}{2c(4m_0E)^{1/2}} \frac{1}{(\alpha_{11} + 3\alpha_{22})^{1/2}} \times [(4\alpha_{11}\alpha_{22} + \alpha_{11}\alpha_{33} + 3\alpha_{22}\alpha_{33} - 3\alpha_{23}^2) + (4\alpha_{11}\alpha_{22} - \alpha_{11}\alpha_{33} - 3\alpha_{22}\alpha_{33} + 3\alpha_{23}^2) \cos 2\theta - 4\alpha_{11}\alpha_{23} \sin 2\theta]^{1/2}. \quad (1b)$$

For $q||y$, $\theta = 0$ is $H||x$ (binary axis),

$$\Delta\left(\frac{1}{H}\right)_1 = \frac{e\lambda}{2c(4m_0E)^{1/2}} \frac{1}{(\alpha_{22})^{1/2}} [(\alpha_{11}\alpha_{22} + \alpha_{22}\alpha_{33} - \alpha_{23}^2) + (\alpha_{22}\alpha_{23} - \alpha_{23}^2 - \alpha_{11}\alpha_{33}) \cos 2\theta]^{1/2}, \quad (2a)$$

$$\Delta\left(\frac{1}{H}\right)_{2,3} = \frac{e\lambda}{2c(4m_0E)^{1/2}} \frac{1}{(3\alpha_{11} + \alpha_{22})^{1/2}} \times [(3\alpha_{11}\alpha_{33} + \alpha_{22}\alpha_{33} - \alpha_{23}^2 + 4\alpha_{11}\alpha_{22}) + (3\alpha_{11}\alpha_{33} + \alpha_{22}\alpha_{33} - \alpha_{23}^2 - 4\alpha_{11}\alpha_{22}) \cos 2\theta \pm 4\sqrt{3}\alpha_{11}\alpha_{23} \sin 2\theta]. \quad (2b)$$

For $q||z$, $\theta = 0$ is $H||x$,

$$\Delta\left(\frac{1}{H}\right) = \frac{e\lambda}{2c(4m_0E)^{1/2}} \frac{1}{\alpha_{33}^{1/2}} [(\alpha_{11}\alpha_{33} + \alpha_{22}\alpha_{33} - \alpha_{23}^2) + (\alpha_{22}\alpha_{33} - \alpha_{23}^2 - \alpha_{11}\alpha_{33}) \cos 2\theta]^{1/2}, \quad (3)$$

where the x axis is the binary axis, the y axis is the bisectrix, and the z axis is the trigonal axis. For $q||x$, $\Delta(1/H)$ attains its maximum value when

$$\tan 2\theta = 2\alpha_{23}/(\alpha_{33} - \alpha_{22})$$

and when

$$\tan 2\theta = 4\alpha_{11}\alpha_{23}/(4\alpha_{11}\alpha_{22} - \alpha_{11}\alpha_{33} - 3\alpha_{22}\alpha_{33} + 3\alpha_{23}^2).$$

According to Shoenberg's data, these angles are 35° and -55° . A glance at Fig. 7 shows that $\Delta(1/H)$ is a maximum for an angle of 3° in this experiment, with a maximum error of 2° . Therefore, it is concluded that different carriers are observed in these two experiments. For $q||y$, $\Delta(1/H)$ attains its maximum when $H||x$, which requires

$$\alpha_{22}\alpha_{33} - \alpha_{23}^2 > \alpha_{11}\alpha_{22},$$

which is in complete disagreement with Shoenberg's

results. The interpretation of this data will be discussed later.

For $q||z$, the results, taken in conjunction with Ketterson's¹⁵ experiment, are inconsistent with the data of the other orientations. However, the results are consistent with those of Shoenberg. In this case, the least-squares fit to a formula

$$\Delta(1/H) = [A + B \cos 2\theta]^{1/2}$$

gives

$$\Delta(1/H) = [28.62 \times 10^{-6} + 29.54 \times 10^{-6} \cos 2\theta]^{1/2} \text{ G}^{-1}.$$

Since $A \approx B$, it is clear that only the sum $A + B$ is determined, and, therefore, only one of the parameters of the ellipsoid can be obtained. This parameter is α_{11} , and it is found by using formula (3), which reduces to $\Delta(1/H) = (e\lambda/2c)(\alpha_{11}/2m_0E)^{1/2}$ for $H||y$. It is found that $\alpha_{11} = 16.7$, when E_F is taken to be 18.6×10^{-14} erg.

At this point, the author would like to emphasize that Shoenberg obtained his theoretical fit by assuming m_1 to be small compared with m_2 , m_3 , and m_4 ; or, in terms of α_{ij} , the assumption is that $\alpha_{11}\alpha_{22}$, $\alpha_{11}\alpha_{33}$, and $\alpha_{11}\alpha_{23}$ are much larger than $\alpha_{22}\alpha_{33} - \alpha_{23}^2$. From the period of the dHvA oscillations, one obtains the values of $eh(\alpha_{11}\alpha_{22})^{1/2}/\pi c(2m_0E)$, $eh(\alpha_{11}\alpha_{33})^{1/2}/\pi c(2m_0E)$, and $eh(\alpha_{11}\alpha_{23})^{1/2}/\pi c(2m_0E)$, and from the change of amplitude with temperature, one finds $(\alpha_{11}\alpha_{22})^{-1/2}$. Thus, the experiment determines the absolute value of the Fermi energy and $\alpha_{11}\alpha_{22}$, $\alpha_{11}\alpha_{33}$, and $\alpha_{11}\alpha_{23}$. It is clear that the values quoted for α_{22} , α_{33} , and α_{23} (Shoenberg quotes m_2 , m_3 , and m_4 , but it is a simple matter to transform these into α_{ij}) are completely dependent on the value assigned to α_{11} , which Shoenberg, who could not, of course, determine it experimentally, estimated to be 20.

Datars and Dexter,²² who studied cyclotron resonance

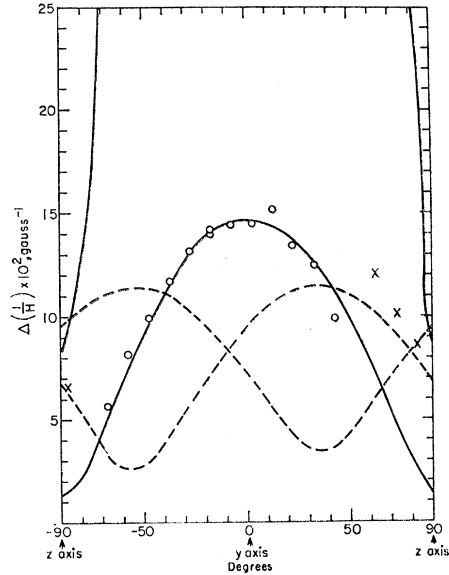


Fig. 8. $\Delta(1/H)$ as function of angle $q||z$; H in yz plane.

²² W. R. Datars and R. N. Dexter, Phys. Rev. **124**, 75 (1961).

in antimony, determined α_{11} by taking into account two of Shoenberg's results. A close examination of the formulas which they used shows that their result for α_{11} is extremely sensitive upon the values assumed for the other parameters. In fact, if the value $(\alpha_{11}\alpha_{22})^{-1/2}=0.095$ is used, the result is $\alpha_{11}=20$, whereas if the value $(\alpha_{11}\alpha_{22})^{-1/2}=0.10$ (as quoted by Shoenberg) is used, α_{11} becomes imaginary. Thus, it is clear that the geometric resonance determination of α_{11} is more accurate, because it is found directly, and not as a combination with other α_{ij} .

Using Shoenberg's experimental data, with the value of α_{11} taken from the geometric resonance results, the parameters become

$$\begin{aligned}\alpha_{11} &= 16.7, \\ \alpha_{22} &= 5.98, \\ \alpha_{33} &= 11.61, \\ \alpha_{23} &= 7.54.\end{aligned}$$

For $q\parallel x$ the least-squares fit to $A+B\cos 2\theta$ gives

$$\Delta(1/H)=[107.6\times 10^{-6}\cos(2\theta-6^\circ)]^{1/2}G^{-1},$$

where θ is measured from the y axis; and for $q\parallel y$ the least-squares fit gives

$$\Delta(1/H)=[77.2\times 10^{-6}+82.7\times 10^{-6}\cos 2\theta]^{1/2}G^{-1},$$

where θ is measured from the x axis.

In the y direction a pure longitudinal wave cannot be propagated in the crystal. However, the transmitting transducer is a longitudinal one, so that it is probable that only a small transverse component is excited. In addition, the receiving transducer is also longitudinal, so that only a small portion of the transverse wave was hardly detectable, and at liquid nitrogen temperature was not detectable at all. The data in this orientation did not differ qualitatively from that in the other orientations (see Fig. 5). For these reasons, it is felt that it is highly improbable that the observed oscillatory behavior of the attenuation is due to the transverse mode. The velocity of sound, which was used to determine the wavelength, was measured at liquid-nitrogen temperature, and, therefore, was the velocity of the longitudinal mode.

In both cases $A\approx B$. If $A>B$ in all directions, then the surface is an ellipsoid; if in any direction $A=B$, it is a cylinder; and if $A<B$ in any direction it is a hyperboloid. Within experimental error ($\sim 5\%$), a significant portion of the Fermi surface is consistent with all three of these possibilities.

In the equations for α_{ij} only the combinations $A\pm B$ occur. Since $A\approx B$, the combination $A-B$ cannot be

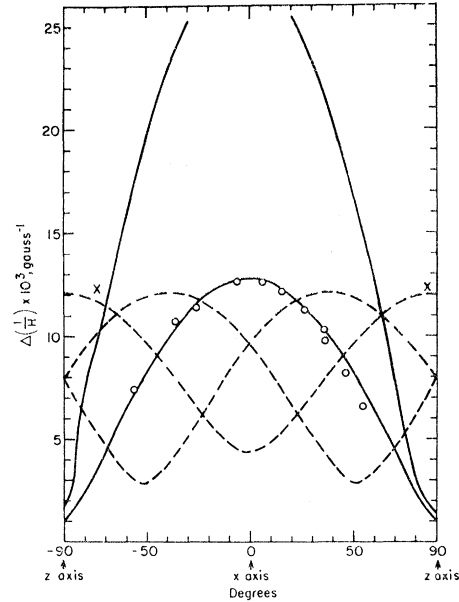


FIG. 9. $\Delta(1/H)$ as function of angle $q\parallel y$; H in xz plane.

used, so we have only three equations for the α_{ij} : two from $\Delta(1/H)$ and one from the tilt angle of 3° when $q\parallel x$.

From the experimental points of Figs. 8 and 9, it is clear that in the x and y directions we follow only one surface. From this data alone it is impossible to choose between the two surfaces of Eq. (1) or between the three surfaces of Eq. (2). This ambiguity is not completely resolved even where the data of the dHvA is taken into account as discussed in II.¹⁵

The solid line in Figs. 6, 7, 8, and 9 are the periods calculated from the first set of α_{ij} given in reference 15. The other possibility discussed there does not give such a good fit in the $q\parallel y$ case but still is consistent with our data. The broken lines are the periods calculated from Shoenberg's data combined with α_{11} derived from this experiment. From these figures it is clear why it is possible to follow only one surface in the $q\parallel x$ and $q\parallel y$ cases.

This experiment cannot distinguish between holes and electrons. As for the Shoenberg carriers the situation is ambiguous: Cyclotron resonance²² experiments identify them as electrons, while galvanomagnetic¹⁸ measurements suggest that they are holes.

ACKNOWLEDGMENTS

The author wishes to express his gratitude to his sponsor, Professor A. W. Lawson, for suggesting the problem and for continued support and encouragement, and to Professor M. H. Cohen for helpful discussions.